

Self-arrangement of cellular circadian rhythms through phase-resetting in plant rootsHirokazu Fukuda,^{1,2,*} Kazuya Ukai,¹ and Tokitaka Oyama^{2,3}¹*Department of Mechanical Engineering, Graduate School of Engineering, Osaka Prefecture University, Sakai 599-8531, Japan*²*PRESTO Japan Science and Technology Agency (JST), 4-1-8 Honcho Kawaguchi, Saitama 332-0022, Japan*³*Department of Botany, Graduate School of Science, Kyoto University, Kitashirakawa-oiwake-cho, Sakyo-ku, Kyoto 606-8502, Japan*

(Received 31 July 2011; published 26 October 2012)

We discovered a striped pattern of gene expression with circadian rhythms in growing plant roots using bioluminescent imaging of gene expression. Our experimental analysis revealed that the stripe wave in the bioluminescent image originated at the root tip and was caused by a continuous phase resetting of circadian oscillations. Some complex stripe waves containing arrhythmic regions were also observed. We succeeded in describing the formation mechanisms of these patterns using a growing phase oscillator network with a phase-resetting boundary condition.

DOI: [10.1103/PhysRevE.86.041917](https://doi.org/10.1103/PhysRevE.86.041917)

PACS number(s): 87.18.Hf, 05.45.Xt, 87.18.Yt

I. INTRODUCTION

The circadian rhythm is an endogenous biological rhythm with an approximately 24 h period. This rhythm is observed in almost all living organisms, including bacteria, fungi, plants, and animals [1,2]. It plays an important role in the optimization of many physiological processes, e.g., gene expression, metabolism, and growth under environmental diurnal cycles. Recent studies have revealed that circadian clocks operate cell-autonomously and that these cellular oscillators are likely to interact with each other in multicellular organisms [3–7]. In plants, spatiotemporal patterns of circadian clock networks have been observed: leaves show a variety of dynamic patterns, including a spiral wave and spatial fluctuation of a phase wave caused by a phase delay along the vein networks [4]. It has been reported that the circadian clock of the shoot is synchronized with that of the root via photosynthesis-related signals from the shoot in diurnal light-dark cycles, while such synchronization becomes unclear under constant light conditions [8]. It has also been reported that plant root branching with a noncircadian period is linked with a traveling wave of oscillating gene expression along the root [9]. These studies imply that the plant root system is involved in physical aspects of nonlinear dynamics as a complex oscillator network [10,11].

A missing link in the understanding of the circadian oscillator network is how newly produced cellular oscillators are coordinated through the proliferation of cells. In plants, cellular oscillators are produced in meristematic tissues and integrated with the whole plant during development, but information on these aspects is completely lacking. We aimed to investigate the formation and coordination of circadian oscillations in newly produced cells in *Arabidopsis* roots using bioluminescence imaging. Cells of elongating roots are primarily produced only at the tip region, and the root itself can be simply modeled as a one-dimensional elongating string [12]. In this paper, we unveil a hidden pattern of circadian oscillation in the root and describe the formation of this pattern using a phase oscillator model.

II. MATERIALS AND METHODS

Experiments were carried out using the transgenic *Arabidopsis thaliana* accession Columbia-0 (Col-0) harboring a *CCA1::LUC* reporter gene [13]. Seedlings were mainly grown at 22 °C for about 1 week on vertical plates (90 × 40 × 10 mm) of 0.4% gellan gum medium containing Murashige and Skoog plant salt mixture supplemented with 2% (w/v) sucrose and 0.1 mM luciferin. The seedlings were grown under 12 h light/12 h dark conditions under fluorescent light (80 $\mu\text{mol m}^{-2}\text{s}^{-1}$) until bioluminescence imaging was performed. Bioluminescence of seedlings was monitored with a highly sensitive EM-CCD camera (Hamamatsu Photonics KK, Japan) in a dark box at 22.0 ± 0.1 °C. Because the gellan gum medium was very clear and had no color, light could fully reach the roots and the bioluminescence from the roots could be observed.

III. EXPERIMENTAL RESULTS

The circadian rhythm in roots of transgenic *CCA1::LUC Arabidopsis* seedlings was observed with bioluminescence imaging [4,7,13–15]. These seedlings carried the firefly luciferase gene under the control of a clock gene promoter, *CCA1*; the luciferase activity oscillated, with a peak at dawn. The phase ϕ of the oscillation denotes the internal biological time, e.g., $\phi = 0$ at the subjective dawn and $\phi = \pi$ rad at the subjective dusk [4].

Under continuous light (LL) or continuous dark (DD) conditions, main and lateral roots formed a striped bioluminescence pattern in the acquired images [Figs. 1(a) and 1(b)]. Since the number of bands in bioluminescence increased by one each day, this hidden pattern can be referred as a *diurnal growth band*. Figure 1(c) shows a space-time plot of bioluminescence images of the main root in Fig. 1(b). The locations of bioluminescence peaks of striped pattern traveled from the base to the tip along the root with a similar velocity to the root growth rate v_R [Fig. 1(c); see Supplemental Material [16]]. Figure 1(c) also shows that any part of the root oscillated with an approximately 24 h period (circadian frequency). The stripe wave did not appear in the initial region ($x \leq x_0$; x indicates the distance from the junction of the root and hypocotyl) that had been entrained directly by light-dark cycles, but emerged in the newly formed regions under constant conditions ($x_0 < x \leq v_R t + x_0$). At

*fukuda@me.osakafu-u.ac.jp

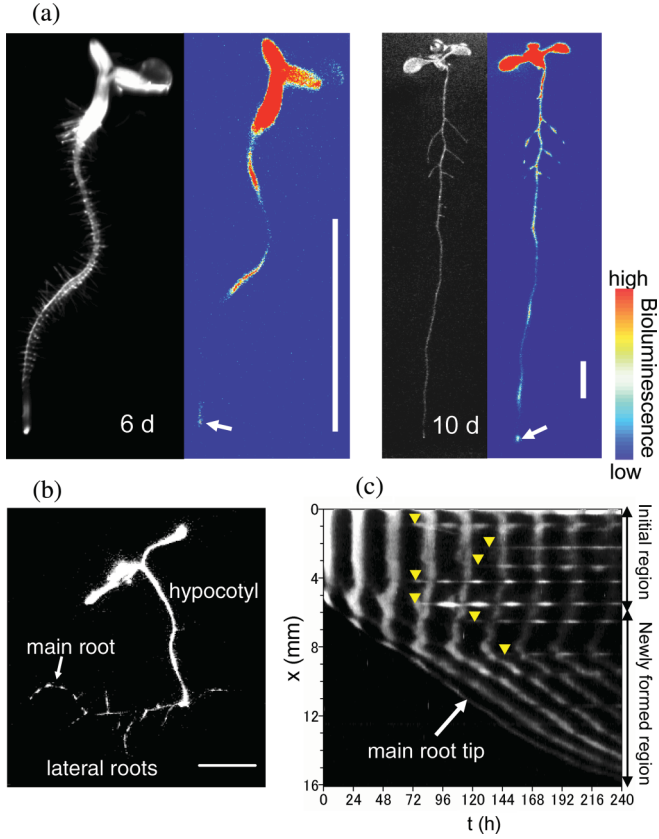


FIG. 1. (Color online) Striped bioluminescence in *Arabidopsis* roots under LL and DD conditions. (a) Bright-field images (left) and bioluminescence images (right) of seedlings at 6 and 10 d after sowing under LL. (b) Bioluminescence image of seedling grown for 8 d under DD. (c) Space-time plot of bioluminescence of the main root in (b), created by tracing bioluminescence along the main root. The gray level indicates the intensity of bioluminescence. The triangles in (c) indicate the starting points of emergence of the lateral roots, in which the following horizontal dotted lines represent the oscillating bioluminescence from the lateral roots. The scale bars indicate 5 mm.

the root tip region, the elongation-differentiation (ED) zones behind the meristematic zone ($x = v_R t + x_0$) showed very weak bioluminescence signal at all times, suggesting that the phase ϕ of *CCA1* oscillation was constantly reset at $\phi|_{x=v_R t+x_0} = \pi$ rad, which could cause a moving boundary condition. Interestingly, detached root tips (>1 mm length) under DD can form the stripe wave [Figs. 2(a) and 2(b)]. Moreover, despite the disruption of the connection between cells by the fragmentation of roots, their bioluminescence seemed to retain a similar pattern to that of intact roots [Figs. 2(c) and 2(d)]. Even in these cases, the traveling velocity of the stripe wave was similar to the root growth rate. This relationship was maintained even when the root growth rate gradually decreased [Figs. 2(b) and 2(d)].

IV. FORMATION MECHANISMS OF SPONTANEOUS PATTERNS

A. Stripe wave

To address the mechanism of formation of the stripe wave, we introduce an oscillator model with the following

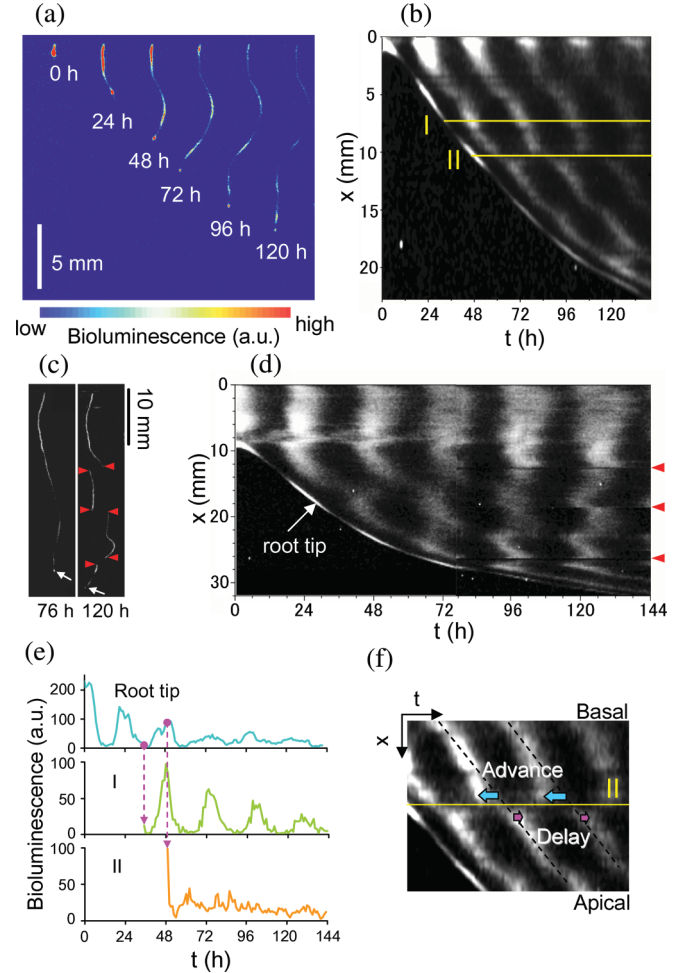


FIG. 2. (Color online) Stripe waves in detached and fragmented roots under DD. (a) Snapshots of bioluminescence in a detached root tip obtained from a 7 d old seedling grown in medium. (b) Space-time plot of bioluminescence of the detached root in (a). (c) Bioluminescence images of a detached root at $t = 76$ and 120 h. At $t = 76$ h, the root was cut into four pieces. Arrows and triangles indicate the root tip and the cutting positions, respectively. (d) Space-time plot of bioluminescence of the detached root in (c). Triangles indicate the cutting positions. (e) Bioluminescence at the meristem in the root tip, rhythmic region (I), and arrhythmic region (II) in (b). (f) Enlarged illustration of space-time plot around II in (b).

assumptions. First, under constant conditions, seedlings do not require any signals to entrain the cellular oscillators from the external environment. Second, because detached roots under DD form a stripe wave (Fig. 2), entrainment signals from the shoot to the roots are nullified for its formation. Finally, every region of roots shows the self-sustained oscillation because fragmented roots seem to retain a similar bioluminescence, despite the disruption of the coupling between cells along the shoot-root axis [Fig. 2(d)]. Therefore, the circadian clock system in roots under constant conditions can be approximately described by a simple phase oscillator model that represents only *cell-autonomous oscillation*:

$$d\phi_j/dt = \omega, \quad (1)$$

where ϕ_j is the phase of cell j along the root and ω is the circadian frequency. Simulations were performed under

a moving boundary condition, which was described by $\phi_{j^*}^{(m,n)} = \pi$ rad, where j^* and s refer to the boundary cell and the length of each cell, respectively. The notation $[\]$ indicates a floor function. We reproduced the stripe waves by computations using the simple phase oscillator model [Eq. (1)] with various values for root elongation velocity, v_R . The wavelength of the stripe wave, l_p , the distance between peaks in the striped bioluminescence, depends on v_R according to $l_p = 2\pi v_R/\omega$. Therefore, l_p varies widely depending on the growth rate, as shown in Fig. 2(d). This result suggests that the stripe wave in the root is fundamentally different from ordinary traveling waves in chemical oscillator systems, such as the trigger waves in the Belousov-Zhabotinsky reaction, which have almost constant traveling velocity and constant wavelength of its pattern as strongly determined by diffusion coefficient and the rate of autocatalysis [17,18].

B. Arrhythmicity in stripe wave

The simple mathematical simulation with Eq. (1) suggests that the principal factor for the formation of the stripe wave is the phase resetting of circadian oscillations at the ED zone. In this model, cellular oscillations in the meristematic zone at the very root tip are ignored; the actual root showed a damped oscillation in that zone during growth under constant conditions [Fig. 2(e)]. Furthermore, although the simple phase oscillator model with a moving boundary condition fit the basic pattern formation of the stripe wave, the stripe wave in actual roots often involved some regions with irregular rhythmicity, such as the slip at the region II in Fig. 2(b). This region seemingly included an arrhythmic point showing a constant bioluminescence. We found that the arrhythmic regions could originate only from the oscillatory meristem, keeping a clear bioluminescence oscillation, but not from the static meristem with almost constant bioluminescence [for example, after 120 h in Fig. 1(c)]. We also found that the arrhythmic regions originated from the meristematic zone only when it was showing a peak in bioluminescence rhythm ($\phi \sim 0$ rad) [II in Fig. 2(e)]. This suggested that the initial phase of cellular circadian clock at the entry into the following ED zone influenced the resetting of the clock there [Fig. 2(e)]. Interestingly, divergent phase drifts (phase slip) were observed in the region: the phase advance occurred on the basal side of the arrhythmic region (II), and the phase delay occurred on the opposite side [Fig. 2(f)]. This result implies that the phase-resetting force may be described by a sinusoidal function. Thus it is likely that cellular oscillators in the arrhythmic regions suffered a desynchronizing perturbation at the time they were in the ED zone. Moreover, the coupling between cells plays an important role in maintaining the stripe wave, because a phase shift emerged after the cutting of the root, as shown in Fig. 2(d).

To verify the mechanism of formation of the arrhythmic region, we introduced a three-dimensional coupled oscillator model with a term for phase resetting in the ED zone:

$$\begin{aligned} \frac{d\phi_j^{(m,n)}}{dt} = & \omega_j^{(m,n)} + \delta_{jk} C \sin(\pi - \phi_j^{(m,n)}) \\ & + K \sum_{\langle l,p,q \rangle} \sin(\phi_l^{(p,q)} - \phi_j^{(m,n)}), \end{aligned} \quad (2)$$

where $\phi_j^{(m,n)}$ and $\omega_j^{(m,n)}$ represent, respectively, the phase and circadian frequency of the cell located at position (m,n) of section j along the root. We considered a cellular system composed of $N_m \times N_n$ cells (section size) $\times N_j$ cells (root length). The term $\delta_{jk} C \sin(\pi - \phi_j^{(m,n)})$ represents the force of phase resetting, where k indicates the cells in the ED zone, C is the strength of the phase resetting, and δ_{jk} is Kronecker's delta. This force also induces both the converse (synchronization) and diverse (desynchronization) effects of the oscillators, depending on $\phi_j^{(m,n)}$. The simulations were performed using Eq. (2) under a moving boundary, which is denoted $j^* = [(v_R t + x_0)/s]$. Regarding cell proliferation in the meristem, we suppose that daughter cells inherit the phases of their parental cells with stochastic noise $\phi_{j^*}^{(m,n)} = \phi_{j^*-1}^{(m,n)} + \epsilon$, where ϵ is a random phase-copying error, which is distributed normally with mean $\langle \epsilon \rangle = 0$ and standard deviation σ_ϵ . The force of phase resetting, which is described as the second term in Eq. (2), operates only in the ED zone ($j^* - c_1 - c_2 \leq j < j^* - c_1$), where c_1 and c_2 represent the sizes of the meristematic and ED zones, respectively. The natural frequency of the j th cell $\omega_j^{(m,n)}$ is distributed normally

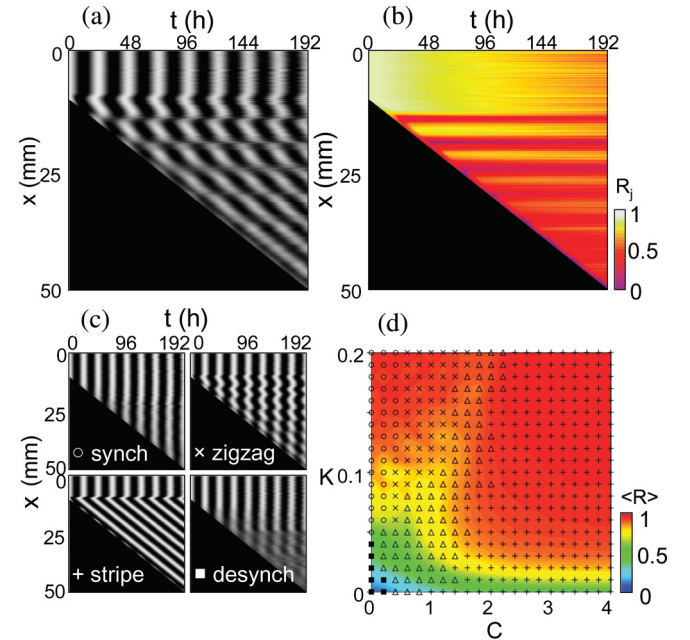


FIG. 3. (Color online) Complex stripe waves obtained by computer simulations. (a) Space-time plot of bioluminescence X_j in the stripe wave with some arrhythmic regions (slips). In this plot, $K = 0.02$ and $C = 0.8$. (b) Space-time plot of synchronization index R_j for (a). (c) Completely synchronized ($K = 0.1, C = 0$), zigzag ($K = 0.1, C = 0.6$), stripe ($K = 0.1, C = 3$), and desynchronized ($K = 0.03, C = 0$) patterns. (d) Diagram for the patterns in (c) and the averaged synchronization index $\langle R \rangle$. $\langle R \rangle$ is the average of R_j among newly formed region at $t = 192$ h. Symbols indicate completely synchronized (\circ), zigzag (\times), stripe ($+$), and desynchronized (\blacksquare) patterns, and stripe pattern with slips (\triangle). In this simulation, $\bar{\omega} = 2\pi$ rad/d, $\sigma_\omega = 0.05\bar{\omega}$, $\sigma_\epsilon = 0.05/2\pi$ rad, $x_0 = 10$ mm, $c_1 = 5$, $c_2 = 5$, $N_m = 10$, $N_n = 10$, $v_R = 0.28$ mm/h, and $s = 0.1$ mm. All numerical simulations were performed using the fourth-order Runge-Kutta method with a time step of 0.01.

with average $\bar{\omega}$ and standard deviation σ_{ω} . In addition, the third term in Eq. (2) is the coupling between cellular oscillators, where $\sum_{\langle l,p,q \rangle}$ means summation over the nearest neighbors of the cell in the position (m,n) at section j .

Figure 3(a) shows a stripe wave with arrhythmic regions (slips) in its bioluminescence X_j [$X_j = 1/N \sum_{m,n} \cos(\phi_j^{(m,n)})$, where $N = N_m \times N_n$]. In this simulation, arrhythmic regions originated from the meristematic zone (root tip) showing a peak bioluminescence. As expected, after the bioluminescence oscillation at the meristematic zone was damped by desynchronization of the cellular rhythms, the arrhythmic region did not form [Fig. 3(a)]. Figure 3(b) shows a space-time plot of the synchronization index R_j [$R_j = 1/N |\sum_{m,n} \exp(i\phi_j^{(m,n)})|$] for the population of cells in each section. Because R_j values at arrhythmic regions are low, the arrhythmia was caused by desynchronization between cells in sections. In addition to this slip pattern [Fig. 3(a)], four other patterns (completely synchronized, zigzag, stripe, and desynchronized patterns) were observed in our simulations [Fig. 3(c)]. Figure 3(d) shows a diagram for such patterns and the average synchronization index $\langle R \rangle$ as a function of C and K . For sufficiently large C , the striped pattern emerged widely in both uncoupled ($K = 0$) and coupled ($K = 0.2$) conditions. With decreasing C , the pattern changes from a stripe to a slip, zigzag, and completely synchronized pattern at higher values of K . In Fig. 3(d), completely synchronized and zigzag patterns require sufficiently large coupling ($K \geq 0.05$) to emerge. Since we have observed the zigzag-like pattern in experiments such as $t = 72$ h in Fig. 2(d), the root cellular oscillators may be coupled to each other with a certain strength.

V. SUMMARY AND DISCUSSIONS

Our experimental and theoretical analyses on the patterning of the circadian rhythm along roots unveil a way of establishing an array of cellular oscillations in their growth as follows. First, the principal factor for the formation of the stripe wave is the phase resetting of circadian clocks at the root tip. Second, the coupling of cells is not necessary for the formation of the stripe wave [Fig. 3(d)]. However, our results suggest that coupling between cells exists in roots. Finally, from our mathematical

simulations, arrhythmic behavior with the slip pattern in the stripe wave may be generated by desynchronization of cellular oscillators that is caused by a phase-resetting perturbation in the ED zone. The mechanism of the phase-resetting was not revealed, but related information has been reported recently [19]. Distribution of reactive oxygen species in the root tip was shown to be important for the transition from cell proliferation to differentiation, and a DNA-binding transcription repressor, UPB1, was identified as a key factor expressed in the transition zone. It is noteworthy that many genes were identified as its downstream targets and that UPB1 binds to the *CCA1* locus. These dramatic transcriptional changes may result in the cessation of circadian oscillation in this region.

Phase-resetting of circadian clocks through proliferation and differentiation has also been observed in mammalian embryonic stem cells [20], and thus the phase resetting of newly formed cells and tissues appears to play an important general role in initializing developmental processes [9]. The branching formation of lateral roots as repeating units along the root primary axis may be related to the phase resetting of the circadian rhythm, because the phase of lateral roots at their emergence was antiphase to that of the main roots [as shown in Fig. 1(c)]. In addition, at first glance, our observed stripe wave is similar to other growing patterns such as vertebrate segmentation, but the mechanisms controlling them are different [21]. Moreover, in our experiments, cell-autonomously circadian oscillation in roots seems to be strongly enhanced by sucrose in the medium, while the roots of plants cultivated in soil depend on a source of photosynthate from their shoots [8]. Spatiotemporal patterns of circadian oscillation in these different situations will be addressed in future work. In summary, root essentially possesses cell-autonomous circadian oscillations and can arrange them by phase resetting at the growing point.

ACKNOWLEDGMENTS

We are grateful to Dr. N. Nakamichi for supply of *CCA1::LUC* plants, Professor H. Daido, Dr. T. Mizuguchi, and Dr. H. Kori for discussions, and Y. Fukuda for technical assistance.

-
- [1] S. M. Reppert and D. R. Weaver, *Nature (London)* **418**, 935 (2002).
 - [2] C. R. McClung, *Plant Cell* **18**, 792 (2006).
 - [3] S. C. Thain, A. Hall, and A. J. Millar, *Curr. Biol.* **10**, 951 (2000).
 - [4] H. Fukuda, N. Nakamichi, M. Hisatsune, H. Murase, and T. Mizuno, *Phys. Rev. Lett.* **99**, 098102 (2007).
 - [5] M. Doi, A. Ishida, A. Miyake, M. Sato, R. Komatsu, F. Yamazaki, I. Kimura, S. Tsuchiya, H. Kori, K. Seo, Y. Yamaguchi, M. Matsuo, J.-M. Fustin, R. Tanaka, Y. Santo, H. Yamada, Y. Takahashi, M. Araki, K. Nakao, S. Aizawa, M. Kobayashi, K. Obrietan, G. Tsujimoto, and H. Okamura, *Nat. Commun.* **2**, 327 (2011).
 - [6] H. Fukuda, I. Tokuda, S. Hashimoto, N. Hayasaka, *PLoS One* **6**, e23568 (2011).
 - [7] B. Wenden, D. L. K. Toner, S. K. Hodge, R. Grima, and A. J. Millar, *Proc. Natl. Acad. Sci. USA* **109**, 6757 (2012).
 - [8] A. B. James, J. A. Monreal, G. A. Nimmo, C. L. Kelly, P. Herzyk, G. I. Jenkins, and H. G. Nimmo, *Science* **322**, 1832 (2008).
 - [9] M. A. Moreno-Risueno, J. M. Van Norman, A. Moreno, J. Zhang, S. Ahnert, and P. N. Benfey, *Science* **329**, 1306 (2010).
 - [10] A. Pikovsky, M. Rosenblum, J. Kurths, *Synchronization - A Universal Concept in Nonlinear Sciences* (Cambridge University Press, Cambridge, UK, 2001).
 - [11] A. Arenas, A. Díaz-Guilera, J. Kurths, Y. Moreno, and C. Zhou, *Phys. Rep.* **469**, 93 (2008).
 - [12] N. Yazdanbakhsh, R. Sulpice, A. Graf, M. Stitt, and J. Fisahn, *Plant Cell Environ.* **34**, 877 (2011).
 - [13] N. Nakamichi, S. Ito, T. Oyama, T. Yamashino, T. Kondo, and T. Mizuno, *Plant Cell Physiol.* **45**, 57 (2004).

- [14] A. J. Millar, I. A. Carré, C. A. Strayer, N.-H. Chua, and S. A. Kay, *Science* **267**, 1161 (1995).
- [15] S. C. Thain, G. Murtas, J. R. Lynn, R. B. McGrath, and A. J. Millar, *Plant Physiol.* **130**, 102 (2002).
- [16] See Supplemental Material at <http://link.aps.org/supplemental/10.1103/PhysRevE.86.041917> for the movie of the stripe wave formation in roots of a seedling.
- [17] Y. Kuramoto, *Chemical Oscillations, Waves, and Turbulence* (Springer, Berlin, 1984).
- [18] H. Fukuda, N. Tamari, H. Morimura, and S. Kai, *J. Phys. Chem. A* **109**, 11250 (2005).
- [19] H. Tsukagoshi, W. Busch, and P. N. Benfey, *Cell* **143**, 606 (2010).
- [20] K. Yagita, K. Horie, S. Koinuma, W. Nakamura, I. Yamanaka, A. Urasaki, Y. Shigeyoshi, K. Kawakami, S. Shimada, J. Takeda, and Y. Uchiyama, *Proc. Natl. Acad. Sci. USA* **107**, 3846 (2010).
- [21] K. Uriu, Y. Morishita, and Y. Iwasa, *J. Theor. Biol.* **257**, 385 (2009).